Non-Model-Based Observer for Friction Compensation in Servo Drive Position Tracking

T. Dumitriu, M. Culea, Tr. Munteanu, E. Ceangă
"Dunărea de Jos" University, ISCEE Department, Galați, ROMÂNIA

Abstract **- Friction is to be considered an essential process for micrometer scale tracking servo systems. Therefore, a high performing and robust control of friction becomes an important issue in mecatronics and robotics field of research. In this paper, considering the LuGre model of friction, a non-model-based friction compensator is proposed to improve position tracking in a DC electrical drive system. The approach to friction influence compensation is based on the disturbance observer. Friction is to be considered as a load torque for the DC drive took into account and will be estimated via three different structures proposed by the authors. Afterwards, the observer is implemented in a classical feedback compensation scheme in which friction is treated as a load disturbance torque. The efficiency of using such observers in DC servo drive with friction is analyzed by computer simulation of a position control system.**

Index of terms **- stick-slip motion, stiction, LuGre friction model, limit cycles, model-based compensation, PID control.**

I. Introduction

Disturbance torques, among friction is the most frequent, are present in almost every motion control applications. In position and speed control systems with high accuracy requirements friction torque has a strong negative effect on the desirable control quality. Static friction (stiction) effect in standstill, Coulomb friction, nonlinearity and negative derivation of static characteristic of friction during transition from stiction to Coulomb friction, called Stribeck curve are features that made friction to be responsible for several servomechanism problems. Tracking errors, limit cycles and undesired stick-slip motion are the most known phenomena that friction can lead to. Control strategies that attempt to compensate for the effects of friction are described in [1], [6]. As a thumb rule, the compensation approaches are classified in model-based and non-model-based techniques [8].

A. Model-based approach

Its implementation requires choosing the appropriate friction model, identification of its parameters, and finally friction compensation using the identified model. This also assumes that the force or torque actuation of adequate bandwidth is available and stiffly coupled to the friction element. Then, friction compensation can be obtained by adding the opposite of the predicted friction to the control signal (see section 3).

B Non-model-based approach

In this case no friction model is used and the compensation is achieved by:

1) Changing the position controller parameters;
2) Applying dither;
3) Using a non-model-based observer for friction.

This paper deals with third of the methods mentioned above proposing three different structures for friction observer, each one treating friction as a load or disturbance torque. Thus, the paper is organized like in following. In section 2 the LuGre friction model is presented as a complete dynamic model, which captures most of the friction behavior that has been observed experimentally, in order to justify the authors' choice in friction modeling. In section 3 are presented some feedback and feedforward schemes corresponding to friction compensation techniques. Section 4 is dedicated to disturbance observers proposed and developed by authors for a DC servo drive system with friction while the latter sections are focused on simulation results and conclusions presentation.

II. Friction modeling

Friction is a natural phenomenon that is quite hard to model, and it is not completely understood. The classical friction models are described by static maps between velocity and friction force. Typical examples are different combinations of Coulomb friction, viscous friction, and Stribeck effect. The latter is recognized to produce a destabilizing effect at very low velocities [1]. The classical models explain neither hysteretic behavior when studying friction for nonstationary velocities nor variations in the break-away force with the experimental condition or small displacements that occur at the contact interface during stiction – the so-called Dahl effect. Therefore, friction must be modeled including dynamics for a better accuracy in describing friction phenomena. It is important to underline that the more important purpose pursued in conceiving or adopting a friction model is to capture the friction phenomena for low velocities and especially for crossing zero velocity regime. However, one of the first dynamical models for friction was proposed by Dahl [5]. Describing the spring-like behavior of friction during stiction, the model is essentially Coulomb friction with a lag in the change of friction force when the direction of motion is changed. Thus, the friction force is only a function of the displacement and the sign of velocity. This implies that the friction force is

only position dependent and yields a generalization of ordinary Coulomb friction. Unfortunately, the Dahl model neither captures the Stribeck effect, which is a rate dependent phenomenon, nor does it capture stiction. These are the main motivations for the recent extensions of the model.

An attempt to incorporate Stribeck effect into the Dahl model was done by introducing a second-order Dahl model using linear space invariant descriptions [2]. The new model, called Bliman-Sorine, describes the friction as a function of the path only and it does not depend on how fast the system moves along it. Expressed as a linear system in the space variable $s = \int_0^t |v(\tau)| d\tau$, the model can be viewed as a parallel connection of a fast and a slow Dahl model. The fast model has higher steady state friction than the slow model. The force from slow model is subtracted from the fast model, which results in a stiction peak. Therefore, the friction peak mentioned above emulates quite accurately the equivalent of stiction for a dynamic model but does emulate the Stribeck effect only at a certain distance after motion starts.

The essential elements of the concepts presented so far have been lately integrated in the friction model aiming to establish a link between tribology (all mechanical aspects of contacting surfaces) and modeling for control [3]. Named LuGre model of friction (abbreviation from Lund and Grenoble), the model is related to the bristle interpretation of friction. It includes Stribeck effect, rate dependent friction phenomena such as varying break-away force and frictional lag. Friction is modeled as the average deflection force of elastic springs associated to the contact. When a tangential force is applied, the bristles will deflect like springs. If the deflection is sufficiently large the bristles start to slip. The average bristle deflection (the new state of friction process - z) for a steady state motion is determined by velocity. It is smaller at low velocities, which implies that the steady state deflection decreases with increasing velocity. The model has the form:

$$\frac{dz}{dt} = v - \frac{\sigma_0 |v|}{g(v)} z \tag{1}$$

$$F = \sigma_0 z + \sigma_1 \dot{z} + \alpha_2 v \tag{2}$$

where z is the pre-sliding displacement or, more accurately, the average deflection of the bristles, σ_0 and σ_1 are the stiffness of bristle and, respectively, the damping, α_2 is viscous friction. The function $g(v)$ is the function describing Stribeck's effect. A parameterization proposed for $g(v)$ is given hereafter:

$$g(v) = F_C + (F_S - F_C) e^{-(v/v_S)^2} \tag{3}$$

where F_C is Coulomb force, F_S static friction and v_S is Stribeck's velocity. The Bliman-Sorine (B-S) and the LuGre models are both extensions of the Dahl model, both attempting to capture the stiction phenomenon in two different ways: either by using a two Dahl models in parallel (B-S) or by introducing a velocity varying coefficient, σ_1 (LuGre). Whereas the LuGre model includes the Stribeck effect and also offers a smooth transition at velocity reversal, the reason of its choice for next investigations in control of systems with friction is fully justified. Fig.1 illustrates the LuGre model of friction implemented in MATLAB/Simulink® as a tool for further analysis of friction compensation and control for high precision positioning applications.

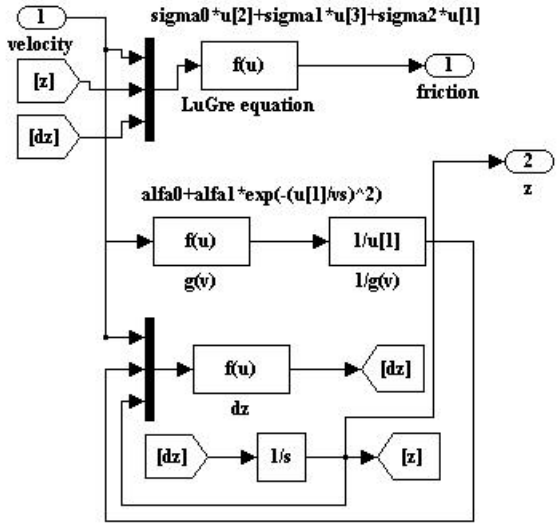

Fig. 1. Simulink® LuGre friction model

III. Friction compensation

There are many ways to compensate for friction [5]. A very simple way to eliminate some effects of friction is to use a dither signal that is a high frequency signal added to the control signal. The effect of the dither is that it introduces an extra force which makes the system moves before the stiction level is reached – the effect is thus similar to removing stiction.

Systems for motion control typically have a structure with a current loop, a velocity loop and a position loop. Since friction appears in the inner loop it would be advantageous to introduce friction compensation in that loop. To obtain effective friction compensation it is necessary to measure or to estimate the velocity is with a good resolution and small delay. Friction compensation become more difficult if there is considerable dynamics between the control signal and the friction force. All these issues are taking into account in the compensation scheme proposed hereafter. Considering the model choice for friction as a good and appropriate manner to describe with high accuracy the friction phenomena involved in classical electrical drives, first of all a reviewing of main compensation schemes is presented.

The idea for a friction compensator for a position servo

with velocity and position control is quite simple and is depicted in fig.2. The friction force F is estimated using some model, and a signal that compensates the estimated friction force $\hat{F}$ is added to the control signal.

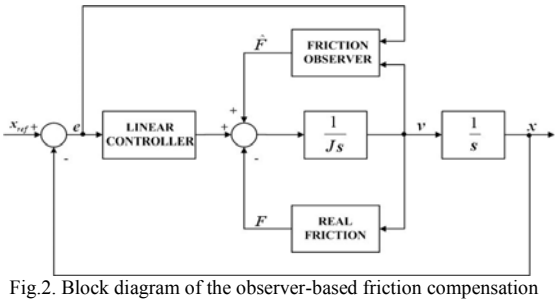

Fig.2. Block diagram of the observer-based friction compensation

For tracking tasks friction can be predicted and partially compensated by feedforward. This has advantage of eliminating the lag and the noise effects of the velocity prediction. It is only suitable for tracking since the desired velocity trajectory is known in advance (fig.3).

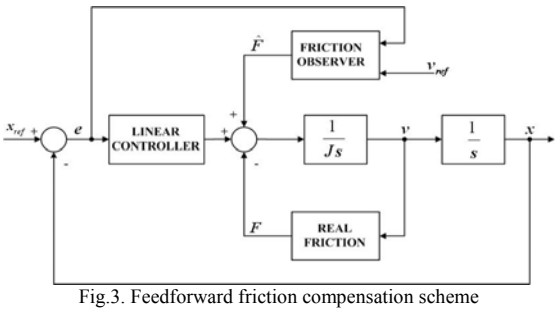

Fig.3. Feedforward friction compensation scheme

The model-based compensation schemes can be classified according to what estimate of velocity is used to evaluate the friction model and what portions of the friction model are applied. Usually, compensation of Coulomb friction is included as well as many additional terms according to extended friction features used.

The friction observer (fig.2 and fig.3) is designed based on friction model adopted for analysis purposes. For LuGre friction model, the observer design is based on passivity theory [2]. It is shown that the system can be decomposed into a standard feedback configuration with a linear block and a nonlinear block. Passivity theory is used to derive the conditions on the controller that guarantees that the closed loop system is stable. The condition is that the resulting linear block is SPR (strictly positive real). For similar circumstances the authors approach is to replace the friction model-based observer with a load torque estimator expressed either in a stochastic manner as a filter or in a determinist conception. The architecture of compensation scheme is presented in fig.4 and its block diagram is available for both mentioned approaches regarding the friction observer structure.

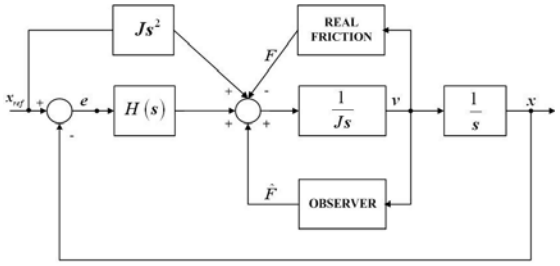

Fig.4. Feedback observer compensation architecture

IV. Friction estimation

Generally, the load torque T_{LOAD} of an electrical drive (DC or AC) is the sum of inertial torque $T_{inertia}$, external torque T_{ext}, and friction torque $T_{friction}$. Considering a classical DC electrical servo drive for a numerical positioning system it could be supposed that the friction torque prevails and the assumption $T_{LOAD} \approx T_{friction}$ works out especially for low velocities and crossing zero velocity regimes. Around this hypothesis the following friction estimator structures are proposed in order to develop the feedback compensation scheme to diminish the negative effects of friction.

A. Filter estimator

The analysis of block diagram in fig.5 which represents the mathematical model of a DC motor shows that the load torque can be estimated, under assumption of speed and current measuring, as follows:

1) according to the shaft rotation speed Ω, the estimator has a PD action with $Js + F_v$ as transfer function; to obtain a strictly causal or a limit causal system corresponding to the Ω input of estimator a proportional strictly causal subsystem $H_0(s)$ must be added to PD component; thus, the response of the estimator will be the same as the one $H_0(s)$ subsystem provides for $T - T_{LOAD}$.

2) according to I_A input, the estimator must behave as a strictly causal system with P action with the same dynamics like $H_0(s)$; the estimator response for I_A input multiplied by magnetic flux torque coefficient K_ϕ will be added with reversed sign to the Ω input response.

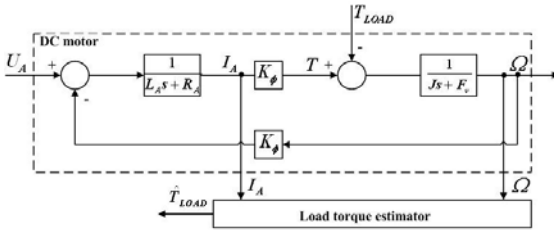

Fig.5. Block diagram of DC motor with load torque estimator

According to the above discussed matters the following

equations hold.

$$H_{\Omega} = -\left(Js + F_v\right) H_0\left(s\right) \tag{4}$$

$$\begin{aligned} \hat{T}_{LOAD}\left(s\right) &= -\left(Js + F_v\right) H_0\left(s\right) \Omega\left(s\right) = \\ &= H_0\left(s\right)\left[T_{LOAD}\left(s\right) - T\left(s\right)\right] \end{aligned} \tag{5}$$

$$H_I\left(s\right) = K_{\phi} H_0\left(s\right) \tag{6}$$

$$\hat{T}_{LOAD} = K_{\phi} H_0\left(s\right) I_A \tag{7}$$

Eq.5 and 7 denote the estimated load torque corresponding to Ω and I_A, respectively, inputs while H_{Ω} and H_I are the transfer functions for each input. The expression of the estimator response when both inputs are applied is:

$$\begin{aligned} \hat{T}_{LOAD} &= H_0\left(s\right)\left[T_{LOAD}\left(s\right) - T\left(s\right)\right] + \\ &+ H_0\left(s\right) T\left(s\right) = H_0\left(s\right) T_{LOAD}\left(s\right) \end{aligned} \tag{8}$$

Thus, beside the transfer function $H_0\left(s\right)$ of the strictly causal subsystem defined before, the dynamic performances of the estimator must be imposed. Subsequently, according to the $H_0\left(s\right)$ order the estimators could be denoted as 1st, 2nd,…, n-th order. The estimator synthesis considers that along the achievement of dynamic performances a good rejection of measurement noise due to current and speed acquisition must be accomplished. Therefore, a low-pass filter (LPF) must be inserted to obtain this estimator response (bold line in fig.6). However, a physical circuit cannot realize this response and the actual response will be in general as shown in fig.6 (dash lines). Hence, the ideal LPF response can be approximated by a rational function approximation such as Butterworth filter. As the filter order grows the approximation gets better. In fig.7 is presented a first order load torque estimator.

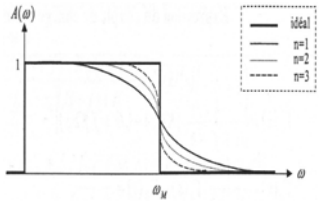

Fig.6. Ideal LPF and Butterworth filter

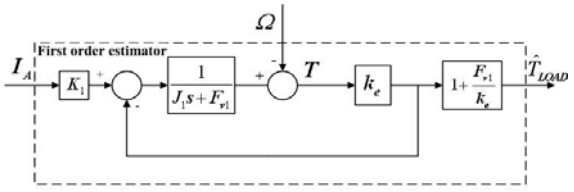

Fig.7. First order load torque estimator

The estimator pass band is imposed by the cutoff frequency ω_M chosen so that a compromise between the acquisition noise level and dynamic performances of the estimator is reached. The following equations describe the estimated torque, assuming that the all parameters involved are already known ($K_1 = K_{\phi}$, $J_1 = J$, $F_{V1} = F_V$):

$$\begin{aligned} \hat{T}_{LOAD}\left(s\right) &= \frac{\left(1 + \frac{F_v}{k_e}\right) k_e}{Js + F_v + k_e}\left[K_{\phi} I\left(s\right) - \right. \\ &\left. - \left(Js + F_v\right) \Omega\left(s\right)\right] \end{aligned} \tag{9}$$

$$\begin{aligned} &\hat{T}_C = H_0\left(s\right) T_C;\ H_0\left(s\right) = \frac{1}{T_0 s + 1}; \\ &T_0 = \frac{J}{k_e + F_v};\ \omega_M = \frac{1}{T_0} \end{aligned} \tag{10}$$

It must be noticed that the viscous friction coefficient will be included in the friction model and obliterated from the DC motor and the torque estimator and observers models.

B. Load torque observer theory applied to DC servo motor

Starting from the model equations of DC motor:

$$\begin{aligned} U_A &= R_A i_A + L_A \frac{di_A}{dt} + K_{\phi} \Omega \\ J \frac{d\Omega}{dt} &= K_{\phi} i_A - T_{LOAD} \end{aligned} \tag{11}$$

the state-space representation is:

$$\begin{aligned} \dot{x} &= Ax + Bu \\ y &= Cx \end{aligned} \tag{12}$$

where:

$$\begin{aligned} &x = \begin{bmatrix} i_A \\ \Omega \end{bmatrix};\ u = U_A; \\ &A = \begin{bmatrix} -\frac{R_A}{L_A} & -\frac{K_{\phi}}{L_A} \\ -\frac{K_{\phi}}{J} & 0 \end{bmatrix};\ B = \begin{bmatrix} \frac{1}{L_A} \\ 0 \end{bmatrix} \\ &y = i_A; \qquad\qquad C = \begin{bmatrix} 1 & 0 \end{bmatrix} \end{aligned} \tag{13}$$

As $\left(A, C\right)$ is observable (the current is measurable), the motor states could be estimated by a state observer governed by:

$$\dot{\hat{x}} = A\hat{x} + Bu + GC\left(x - \hat{x}\right) \tag{14}$$

where $G = \begin{bmatrix} g_1 \\ g_2 \end{bmatrix}$ is the observer gain determined so that the estimation error $e = x - \hat{x}$ tends to 0 faster than the motor's dynamics. From eq.14 the estimation error response using the state equation can be expressed as:

$$\dot{e} = \left(A - GC\right) e \tag{15}$$

For load torque estimation purpose the previous theoretical issues must be extended to a system with disturbances. There are considered two extensions

according to how the disturbance is assimilated: as an unknown input or as a state variable.

B1. Load torque as unknown input

In this case eq. 12 and 13 are rewritten as follows:

$$\dot{x} = Ax + Bu + DT_{LOAD} \tag{16}$$

where x, A, B, u are given by eq. 13 with:

$$D = \begin{bmatrix} 0 \\ -\dfrac{1}{J} \end{bmatrix} \tag{17}$$

Using the observer described by eq. 14, the estimation errors for current and speed (e_{i_A}, e_{Ω}) become:

$$\begin{aligned} \dot{e}_{i_A} &= -\frac{\left(R_A + g_1 L_A\right)}{L_A} e_{i_A} - \frac{K_\phi}{L_A} e_\Omega \\ \dot{e}_\Omega &= \frac{\left(K_\phi + g_2 J\right)}{J} e_{i_A} - \frac{T_{LOAD}}{J} \end{aligned} \tag{18}$$

Adopting a fast observer dynamics $\dot{e} \cong 0$ and resorting to a variable substitution in previous equations system the expression of estimated load torque will be:

$$\hat{T}_{LOAD} = \frac{K_\phi\left(K_\phi - g_2 J\right) + F_v\left(R_A + g_1 L_A\right)}{K_\phi} e_{i_A} \tag{20}$$

B2. Load torque as state variable

Considering the load torque as a disturbance variable state the system order of state-space representation increase and eq.12 and 13 are written as follows:

$$\begin{aligned} \dot{x}_a &= A_a x_a + B_a u \\ y_a &= C_a x_a \end{aligned} \tag{21}$$

where:

$$x_a = \begin{bmatrix} i_A \\ \Omega \\ T_{LOAD} \end{bmatrix};\ A_a = \begin{bmatrix} -\dfrac{R_A}{L_A} & -\dfrac{K_\phi}{L_A} & 0 \\ \dfrac{K_\phi}{J} & 0 & -\dfrac{1}{J} \\ 0 & 0 & 0 \end{bmatrix};$$

$$B_a = \begin{bmatrix} \dfrac{1}{L_A} \\ 0 \\ 0 \end{bmatrix};\ y_a = i_A;\ C_a = \begin{bmatrix} 1 & 0 & 0 \end{bmatrix} \tag{22}$$

The extended observer for this case is depicted now by the modified relation contained in eq.14:

$$\dot{\hat{x}}_a = A_a \hat{x}_a + B_a u + G_a C_a \left(x_a - \hat{x}_a\right) \tag{23}$$

where $G_a = \begin{bmatrix} g_1 \\ g_2 \\ g_3 \end{bmatrix}$ and $\dot{e}_a = \left(A_a - G_a C_a\right) e_a$ is the estimation error state-space equation. The mathematical model of the load torque estimator in the extended version is:

$$\begin{cases} \dot{\hat{x}}_1 = -\dfrac{R_A + g_1 L_A}{L_A} \hat{x}_1 - \dfrac{K_\phi}{L_A} \hat{x}_2 + U_A + g_1 i_A \\ \dot{\hat{x}}_2 = \dfrac{K_\phi - g_2 J}{J} \hat{x}_1 - \dfrac{1}{J} \hat{x}_3 + g_2 i_A \\ \dot{\hat{x}}_3 = -g_3 \hat{x}_1 + g_3 i_A \end{cases} \tag{24}$$

Proceeding in same manner described before and knowing that $\hat{x}_1 = \hat{i}_A;\ \hat{x}_2 = \hat{\Omega};\ \hat{x}_3 = \hat{T}_{LOAD}$ the estimated load torque will be:

$$\hat{T}_{LOAD} = g_3 \int e_{i_A} dt \tag{25}$$

In this case the estimated torque does not depend on current error but on its integral term. Therefore, a poor dynamic performance on torque estimation must be taken into account.

V. Simulation results

First of all, a simulation scheme is used to validate the estimation accuracy for the three types of observer developed and configured in previous section of the paper (filter estimator type and the 2 determinist approaches). In fig.8 it is shown a classical DC motor driven by a sinusoidal reference in the presence of a disturbance torque imposed like a friction torque via LuGre model presented earlier. The authors have emulated the worst working regime for the systems with friction – velocity reversal or zero-crossing velocities – to emphasis the observers' capacity to be tuned properly in order to obtain a further accurate compensation for friction.

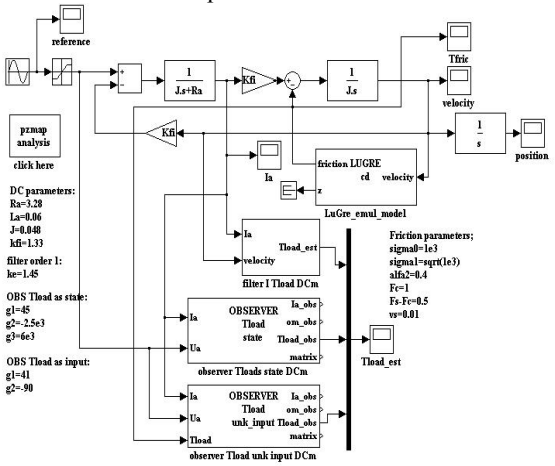

Fig.8. Simulink® scheme for estimated friction torque using a sinusoidal reference for a DC motor

The capture of Simulink® block diagram shown in fig.8 includes the motor parameters as well as the friction model characteristics and observer gains.

In fig.9 are illustrated the simulation results of the system for friction torque, velocity and estimation errors of each observer taken into account.

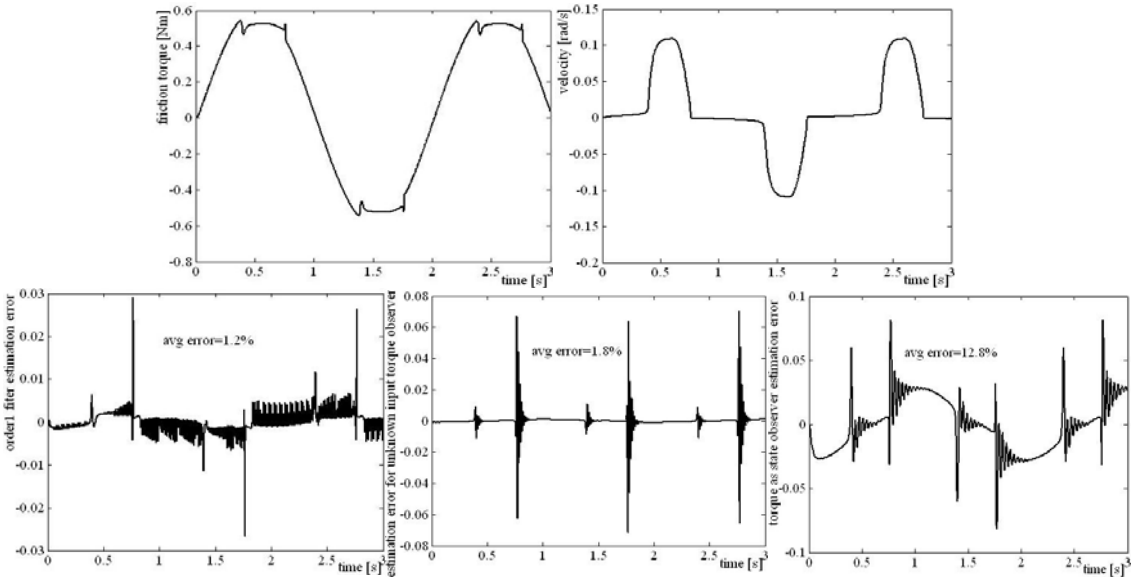

Fig.9. Friction torque (upper left), velocity (upper right) and estimation errors for each observer considered in the system from fig.8

It can be observed a good estimation for the first order torque estimator and for the observer with load torque as unknown input. Moreover, the stick-slip motion and stiction has been pointed out by velocity characteristic.

The next simulations are focused on friction compensation strategy using non-model-based observers. Before using friction compensation, one must analyze its effects in a closed-loop system and avoid situations in which this compensation may result in adverse response characteristics, such as limit cycles.

In fig.10 is presented the model of a tracking servo system that authors have used to illustrate the occurring of limit cycles in servo drives where the controller has integral action.

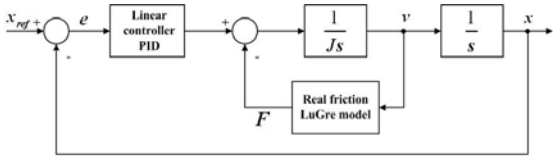

Fig.10. Block diagram for servo limit cycles with PID controller

Choosing the reference position as $x_d = 0.05$ - small tracking scale – the LuGre friction model and its parameters mentioned in fig.8 clearly predict limit cycles as have been experimentally observed in literature [1], [2]. Fig.11 shows the main simulation results for the DC servo drive with a PID controller inducing limit cycles.

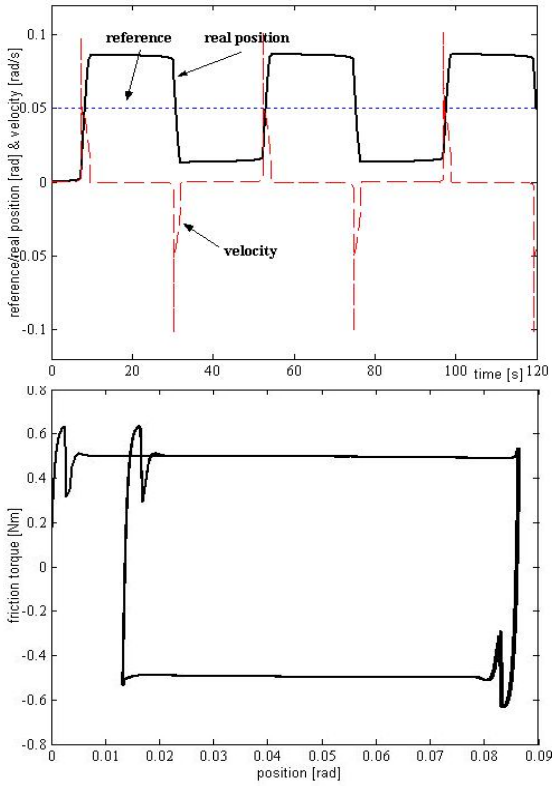

Fig.11. Simulation of PID position control limit cycles: reference position (dotted line), real position (solid line) and velocity (dashed line) – up; friction-position hysteresis for limit cycles – down

The proposed scheme for friction compensation has been

already reviewed in section 3 – fig.4. The block diagram presented herewith depicts a typical closed-loop servomechanism system in which friction compensation has been added. In this system, feedback consists of a state-feedback part ($H(s)$ is a PID controller) and of an off-line non-model-based friction compensation term, $\hat{F}$ (Js^2 as feedforward part is also added to complete a classical feedback compensation strategy).

It must be noticed that the PID controller has a filtered integral action for pole placement and stability reasons. The PID controller tuning rules and observer gains choice has been made according to dynamic constrains imposed for observer response performance versus the transient behavior of DC motor.

Fig.12, 13 and 14 show the position response after compensation applying and also the friction rejection with a detailed zoom-in capture for each observer implemented in the feedback compensation scheme. The PID parameters and observers' gains are also included within figures (tau refer the I filter constant time).

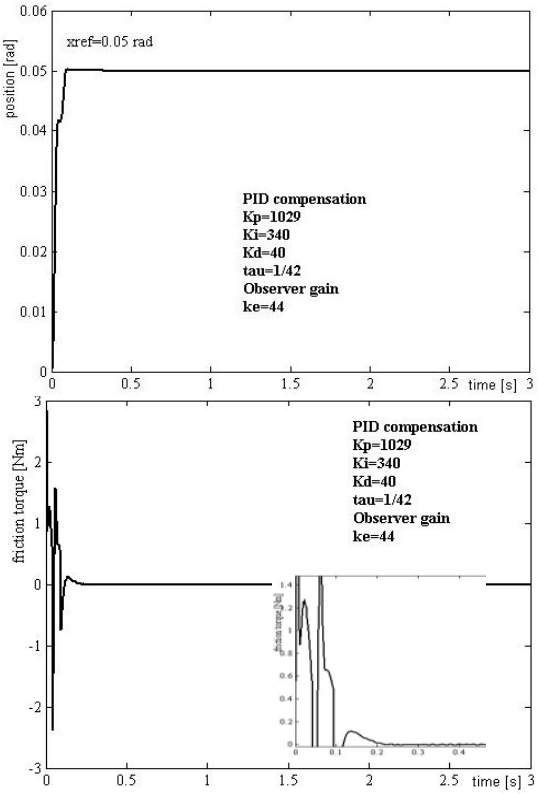

Fig.12. Simulation results (position and friction torque) for a PID compensation strategy using a first order disturbance torque estimator

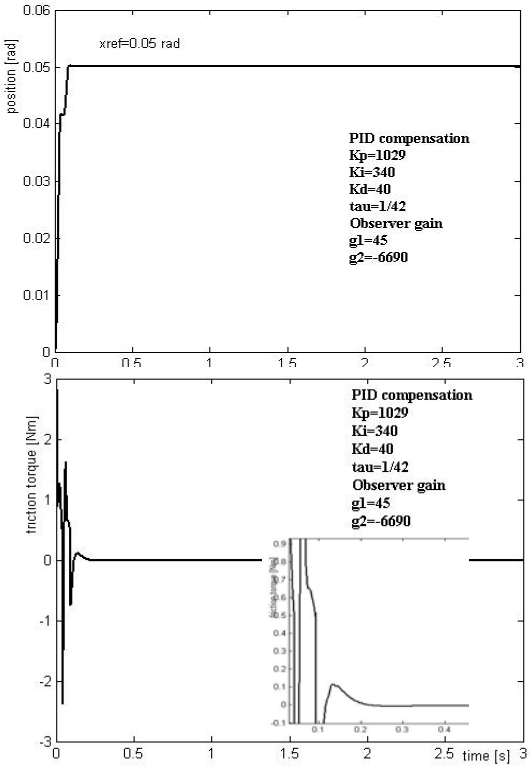

Fig.13. Simulation results (position and friction torque) for a PID compensation strategy using an disturbance observer considering the friction torque as an unknown input

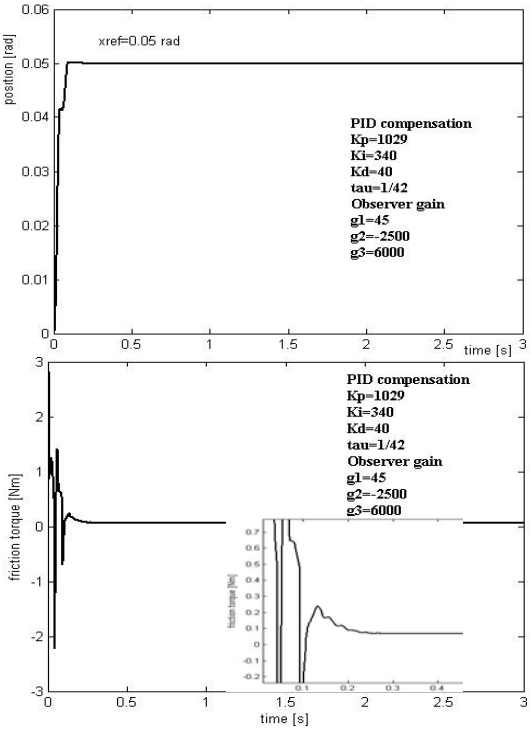

Fig.14. Simulation results (position and friction torque) for a PID compensation strategy using an disturbance observer considering the friction torque as a state variable

It can be observed a good rejection of friction and its effects for the 2 first observers employed and an accurate position tracking for all of them. Despite using high gains in the control loop, the current and speed measurement noise propagated at friction level were easily rejected (it must be also noticed that no current/torque controller has been used – fig.15 illustrates the DC motor current).

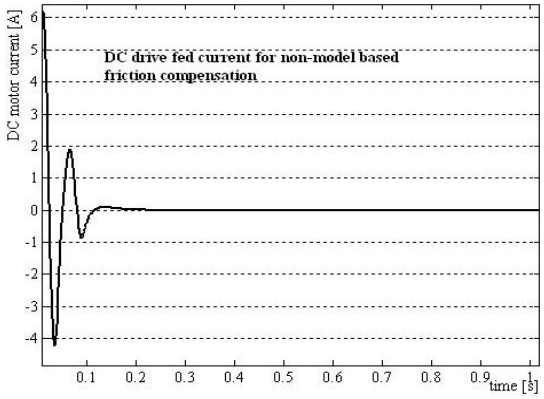

Fig. 15. DC motor fed current for simulation results presented in fig.12 - 14

V. Conclusions

A non-model-based friction compensation method for DC servo drives was described. The advantage of this approach is that it uses load torque observers which don't require a friction model and they can be applied for compensation of various disturbances such as friction.

Other advantage of this control structure is that it realizes a trade-off between a relative simplicity and a good position tracking performances, despite hard nonlinearities involved.

References

[1] Armstrong-Helouvry, B., Dupont, P. and Canudas de Wit, C. *A survey of models, analysis tools and compensation methods for the control of machines with friction*. Automatica, 30(7):1083-1138 (1994).

[2] Bliman, P.-A. and Sorine, M. *Friction modeling by hysteresis operators. Application to Dahl, stiction and Stribeck effects*. Proceedings of the Conference "Models of Hysteresis", Trento, Italy, (1991).

[3] Canudas de Wit, C., Olsson, H., Astrom, K. J. and P. Lischinsky. A *new model for control of systems with friction*. IEEE Trans. Autom. Control, 40(3):419-1425 (1995).

[4] Canudas de Wit, C., Olsson, H., Astrom, K. J. and Sorine, M**.** *Control of systems with dynamic friction.* CCA'99 Workshop on Friction, Hawaii, (1999)

[5] Dahl, P. R. *A solid friction model*. Technical Report TOR-0158 (3107-18)-1, The Aerospace Corporation, El Segundo, CA, (1968).

[6] Olsson, H., Canudas de Wit, C., Gafvert, M., Astrom, K. J. and Lischinsky, P. *Friction models and friction compensation.* Research supported by Swedish Research Council for Engineering Sciences (TFR) under contract 95-759, and partially by EDF under contract P29L13/2L3074/EP663 (1997).

[7] Papadopoulos, E. G. and Chasparis, G. C. *Analysis and model-based control of servomechanisms with friction.* Proceedings of International Conference on Intelligent Robots and Systems – IROS 2002, EPFL Lausanne, Switzerland, 2002.

[8] Voda, A. and Ravanbod-Shirazi, L. *High performance position tracking with friction compensation for an electro-pneumatical actuator***.** CEAI, vol.6, no.2, pp.15-33, 2004.